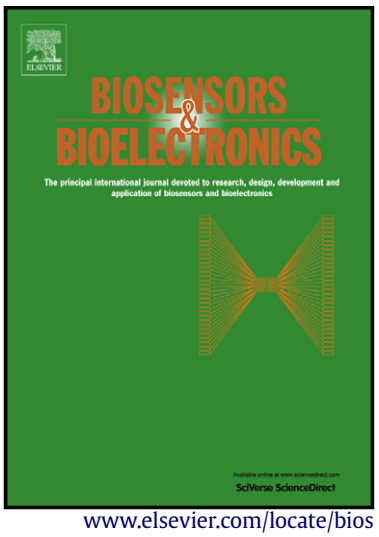

www.elsevier.com/locate/bios

SERS molecular sentinel for the RNA genetic marker of PB1-F2 protein in highly pathogenic avian influenza (HPAI) virus

Yuanfeng Pang, Junfeng Wang, Rui Xiao, Shengqi Wang

PII: S0956-5663(14)00285-1
DOI: http://dx.doi.org/10.1016/j.bios.2014.04.018
Reference: BIOS6722

To appear in: *Biosensors and Bioelectronics*

Received date: 26 January 2014
Revised date: 8 April 2014
Accepted date: 8 April 2014

Cite this article as: Yuanfeng Pang, Junfeng Wang, Rui Xiao, Shengqi Wang, SERS molecular sentinel for the RNA genetic marker of PB1-F2 protein in highly pathogenic avian influenza (HPAI) virus, *Biosensors and Bioelectronics,* http://dx.doi.org/10.1016/j.bios.2014.04.018

SERS molecular sentinel for the RNA genetic marker of PB1-F2 protein in highly pathogenic avian influenza (HPAI) virus

Yuanfeng Pang, Junfeng Wang, Rui Xiao*, Shengqi Wang*

Key Laboratory of New Molecular Diagnosis Techniques for Infectious Diseases, Institute of Radiation Medicine, 27 Taiping Road, Beijing, China

*Correspondent footnote:
Shengqi Wang
Key Laboratory of New Molecular Diagnosis Techniques for Infectious Diseases, Institute of Radiation Medicine, 27 Taiping Road, Beijing, China
Tel: (86)01066930274, e-mail: sqwang@bmi.ac.cn

Rui Xiao
Key Laboratory of New Molecular Diagnosis Techniques for Infectious Diseases, Institute of Radiation Medicine, 27 Taiping Road, Beijing, China

Tel: (86)01066930274, e-mail: ruixiao203@sina.com

Abstract

We have developed a simple and sensitive assay for the detection of the RNA genetic marker associated with high pathogenicity influenza (HPAI) virus. The assay constituted of an array of Raman label tagged hairpin-DNA immobilized on a surface-enhanced Raman scattering (SERS) active substrate as the molecular sentinel (MS) reporter. Upon incubation of the assay with the target RNA, the structure of the hairpin-DNA probe changed from stem-loop configuration (closed state) to DNA/RNA hybridization configuration (open state) so that the Raman label tag will be physically separated from the SERS substrate and induced a decrease of Raman scattering intensity. A metal film over nanosphere (MFON) substrate was developed with a SERS enhancement about 1.7×10^5. Based on this MS-modified substrate, the SERS signal showed a linear relationship to the target RNA in a range of 0-60 attomoles and the limit of detect is 2.67 attomoles. The non-complementary RNA sequences control was also detected and no spectral response was observed. The sensing process only required a single hybridization step and post-hybridization washing can also be omitted. Given that this ultrasensitive biosensor assay is free of polymerase chain reaction (PCR) amplification, it would be a potential diagnostic tool for point-of-care HPAI virus

detection.

Keywords: RNA genetic marker, surface-enhanced Raman scattering, molecular sentinel, point-of-care

1. Introduction

Influenza A viruses is a segmented, negative-strand RNA virus which has been widely studied due to their pandemic potential. Most pandemics have resulted in significant mortality and severe disease among the general population, the most memorable being the Spanish influenza pandemic of 1918 and 1919 (Basler et al., 2008; Beveridge et al., 2000; Smith et al., 2009). These years, highly pathogenic avian influenza (HPAI) H5N1 virus poses a global health concern with new cases continuing to emerge in the human population. The most recent influenza pandemic scare was caused in 1997 by a H5N1 virus originated in Hong Kong (Dybing et al., 2000; Nguyen-Van-Tam et al., 2003; Yuen et al., 1998). Recently, characterization of single-gene reassortants has been identified as a factor responsible for the virulent pathogenicity of HPAI H5N1 virus. More recently, the PB1-F2 protein of the H5N1 virus has been shown to increase pathogenesis with a single amino acid mutation at position 66 (N66S) so that the coding RNA sequence for the amino acid mutation in the PB1-F2 protein is a likely factor to detect and distinguish the HPAI virus with increased pathogenesis from the common influenza virus (Conenello et al., 2007).

Current diagnostic tools available for routine laboratory diagnosis of influenza virus factors rely on the detection of viral nucleic acid by using of amplification techniques, such as reverse-transcription polymerase chain reaction (RT-PCR) assay (Amano et al., 2005; Fouchier et al., 2000). This method can provide a highly sensitive technique in which a very low copy number of RNA molecules can be detected (Arya et al., 2005). However, the exponential growth of the reverse transcribed complementary DNA (cDNA) during the multiple cycles of PCR produces inaccurate end point quantification due to the difficulty in maintaining linearity, resulting of low sensitivity and reproducibility. Moreover, the requirements of expensive equipment, synthetic labeling and professional skills restricted this technology inside the laboratory, so that the development of easy-to-use and self-contained diagnostic tools for influenza point-of-care test was still a challenge.

On the other hand, studies have shown that SERS possesses high sensitivity for the detection of DNA or RNA oligonucleotide sequences based on hybridization of the probe and the target sequences on the SERS-active substrates (Barhoumi et al., 2008; Green et al., 2006; Levin et al., 2009; Wen et al., 2013). Recently, a series of SERS-active substrates such as Au particle-wire, metal film over nanosphere (MFON) and suspended magnetic nanospheres have been developed with giant enhancement factors (EF) for Raman scattering (Kang et al., 2010; Ngo et al., 2013; Wang et al., 2013; Zhou et al., 2013). Due to the “hotspots” scattering on these SERS-active substrates, DNA targets detection with a limit low to 15-20 attomoles

have been reported recently(Li et al., 2013; Wang et al., 2013; Wei et al., 2002). However, SERS biochips reported for RNA targets were not so advanced. Most of the detection methods based on the Raman-labeled nanoparticle probes or Least-Squares analysis with a limit of detect in a sub-nanomolar order (Abell et al., 2012; Negri et al., 2013; Wei et al., 2002). The sensitivity is not sufficient to detect RNAs in clinically relevant samples without an RNA enrichment treatment. For example, to detect circulating miRNAs in blood without PCR enrichment treatment, at least femtomolar sensitivity was needed (Mitchell et al., 2008).

Here, we designed a SERS-based biochip for the RNA marker of HPAIV. An Au-Gr-FON substrate was manufactured as the SERS-active substrate and hairpin-DNA strands with a Raman label molecule Cy-3 at 3′ end were immobilized to the substrate through the 5′ -HS as molecular sentinel (MS) probes. When target RNA was added to the substrate, through the hybridization of the complementary target RNA sequence to the hairpin loop of the MS probe, the stem-loop structure will be opened so that Raman label will be separated from the SERS substrate thus leads to a decreased SERS signal. For the whole detection process, only one-step hybridization was needed and post hybridization washing can be omitted, which making it simple-to-use with short runtime cost and low reagent cost. Compared with the HPAIV factor detection methods reported for which a PCR enrichment treatment was essential for clinically detection (Franks et al., 2006; Kash et al., 2006; Negri et al., 2013), the PCR-free method with high sensitivity and simplicity is more suitable for the point-of-care HPAIV diagnosis.

2. Experimental

2.1. Materials and reagents

Premium precleaned Si wafer was purchased from VWR (Radnor, PA). Mercaptohexanol (MCH), sodium chloride (NaCl), sodium phosphate buffer solution (PBS, pH 7.4) and pretreatment of Si substrates required H_2SO_4, H_2O_2, and NH_4OH were purchased from Sigma Aldrich (St Louis, MO) and used as received unless noted otherwise. Polystyrene beads (PS) (5000 series, size 500nm, CV ≤ 3%, 10% solids) were purchased from Fisher Scientific (Pittsburgh, PA). Millipore Synergy ultrapure water (DI, 18.2 MΩ cm) was used in all aqueous solutions. Colloidal gold and chromium pellets were purchased from Sigma-Aldrich (St. Louis, MO). The buffer and working tools were DNase free. The stem-loop MS probe, the complementary RNA target sequences and the non-complementary RNA for control used in this study were synthesized by Integrated DNA Technologies (IDT, Coralville, IA) and the detail sequences and complementary basepairs information was shown in the Table 1 in Supporting Information. From the analysis of the PB1-F2 protein sequence, RNA sequence coding for a genetic mutation in the influenza PB1-F2 protein (N66S) was used as our target, the MS hairpin-DNA probes were designed with a complementary sequence section to the target RNA for PB1-F2 protein gene mutation strains. The underlined sequences indicate the complementary arms of the MS hairpin, and the bold

sequence represents the sequence complementary to the RNA target in the loop region of the MS hairpin.

2.2. Fabrication of nanoparticle arrays on a Si wafer by nanosphere lithography (NSL) technology.

NSL is a powerful fabrication technique that inexpensively produces nanoparticle arrays with controlled shape, size and inter-particles spacing. In our previous reports, we have used NSL technology to fabricate a series of inverted nanopattern arrays (Wang et al., 2013).The main fabrication procedure was as followed: First, Si substrate was pretreated in two steps (i) piranha etch, 1:3 30% H_2O_2:H_2SO_4 at 80 °C for half an hour (ii) base treatment, 5:1:1 H_2O:NH_4OH:30% H_2O_2 with sonication for 1 h, which rendered the surface hydrophilic. The pretreated substrate was coated by solution casting using approximately 2 μL undiluted nanosphere solution (10% wt/wt%). The nanospheres were allowed to dry in ambient conditions to form a two-dimensional (2D) hexagonally close packed array. Then, the PS colloidal monolayer is etched in oxygen (O_2) plasma to reduce size with inductively coupled plasma (ICP) etching machine (ICP-2B, from Beijing Chuangweina Ltd).

2.3. Deposition of metal film and functionalization of MFON with MS probes.

Au film (200 nm) was evaporated on the substrate coverslips with a thin Cr underlayer (10 nm) for adhesion of Au in a ZZS500 evaporator (from Chengdu Nanguang) with an evaporation rate of 4 Å/s. The MFON substrate was obtained after metal deposition. 0.5 μM MS probes in 20 μL aqueous solution (0.5 M NaCl and 10 mM PBS, pH 7.4) were delivered onto the MFON substrate. The substrate with MS probes was then kept in an airtight container for maintaining a stable humidity. After 2 h, the substrate was rinsed with DI and soaked in 1 mM MCH aqueous solution to displace nonspecifically adsorbed MS probes and to passivate the gold surface. Finally, the substrate was rinsed with DI.

2.4. Monitor the MS probes immobilization and hybridization with RNA target by AFM

After MS probes immobilized on the surface, the substrate was rinsed with DI and RNA samples (20 μL, 500nM in 0.5 M NaCl and 10 mM PBS aqueous solutions, DNase free) was delivered onto MS-immobilized SERS substrates and maintained at 37 °C in an airtight container under constant humidity to promote DNA/RNA hybridization. After 8 h incubation, samples were taken out for detection. The throughout process of the MS probes immobilization and the MS probe/RNA hybridization on the MFON chip was measured by AFM using an Agilent 5500 AFM system equipped with an inverted light microscope (ILM) system. (Agilent, Chandler, AZ)

2.5. SERS sensitivity detection of the RNA target sequences

Samples (50 μL each) of blank and the target RNA (0.5 M NaCl and 10 mM PBS aqueous solutions, DNase free) with different concentrations were delivered onto the MS-immobilized MFON substrates and maintained at 37 °C in an airtight container under constant humidity to promote DNA/RNA hybridization. After 8 h incubation, samples were taken out without washing. Raman measurements were performed using a Raman microscope (BWTEK, Inc., BAC102-785E, United States). A 785 nm near-IR diode laser provided laser excitation. The sample was illuminated through a 20× (N.A. = 0.40) objective resulting in the focused laser spot size, 10 μm in diameter. The laser power used was about 0.36 mW, as measured at the sample. SERS spectra were collected between 2000 and 500 cm^{-1} using a 1s acquisition time with one accumulation.

3. Results and discussion

3.1. The operating and detection principle of the SERS-based MS sensor for RNA

The operating and detection scheme was shown in Fig. 1. First, the PS nanospheres were patterned on the Si wafer and etched in oxygen plasma to increase the space(~ 200nm) between of the PS nanospheres. Then an Au coverslip Cr film was evaporated on the substrate to form the SERS substrate and the gap between of the PS nanospheres decreased to ～50nm. The MS hairpin probes were immobilized on the substrate by using an alkyl thiol substituent at the 5′end. As the 6 basepairs in the arms of the MS probe were complementary so that a stable hairpin structure can be formed through hybridization. The Cy-3 Raman label on the 3′end of the MS hairpin probes was closed to the SERS substrate and induced a strong SERS signal. When the target RNA sequence (with 33 complementary nucleotides to the MS probe starting from 3′end) was added, the hybridization of the RNA with the MS probes will open the stem-loop structure of the probe and separate the Cy-3 dye from the SERS surface and induced a decreased SERS signal.

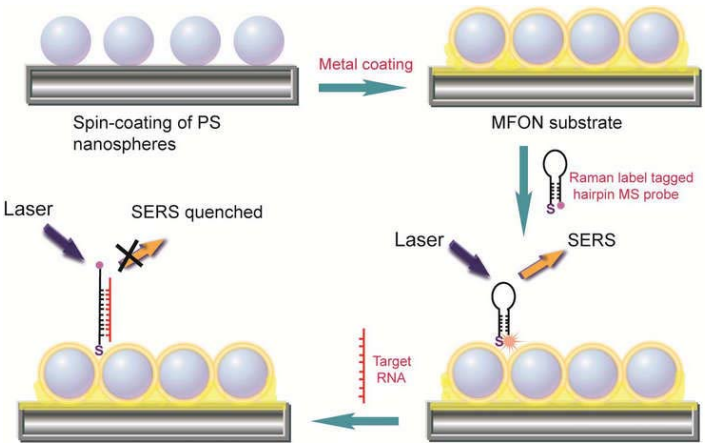

Fig.1. Scheme of the manufacture and detection principle for the RNA marker.

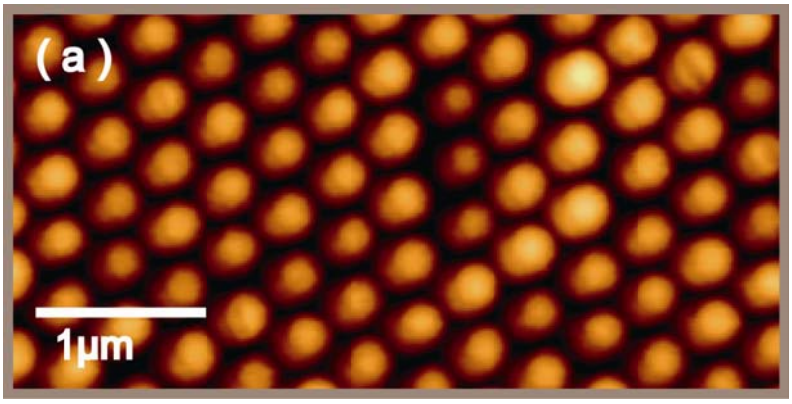

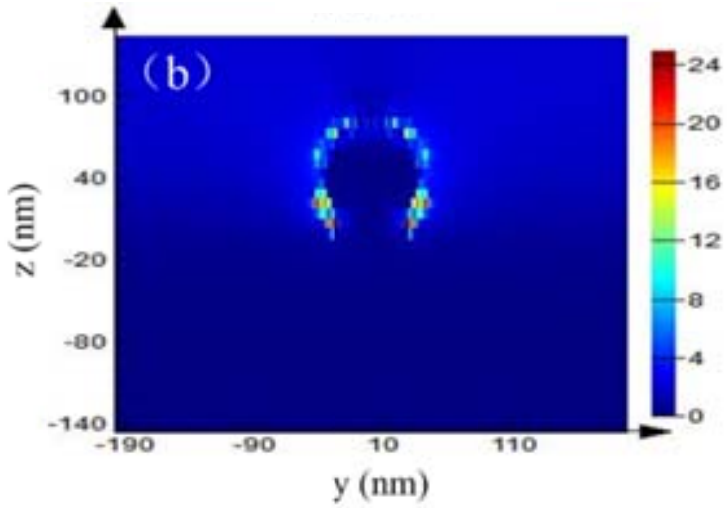

Fig.2. (a) AFM image of the Au-Gr film covered PS monolayer substrate (b) the EM field distribution of the MFON substrate simulated with FDTD method.

3.2. Morphology features and EM distribution of the MFON substrate

The AFM morphology image for MFON chip was presented in Fig. 2a. As it shown, we can obtain the Au-Gr-coated PS nanopattern array on Si substrate with an average diameter 400 nm and the gap between of the nanopattern was ～50nm. To further investigate the enhancement mechanics of the MFON substrate, theoretical calculation was employed to visualize the electromagnetic (EM) field distribution with FDTD method. Theoretical local EM enhancement distribution on the MFON was shown in Fig. 2b. The EM field tends to concentrate at the tips of the Au-Gr-coated PS and form the "hot spots". The largest local EM field enhancement |E| is about 20.50 which created SERS enhancement $|E|^4$ about 1.7×10^5. The result was consistent with the reported MFON substrate's model (Ngo et al., 2013)

3.3. Figurate evaluate and monitor the MS probes immobilization and RNA hybridization event by AFM

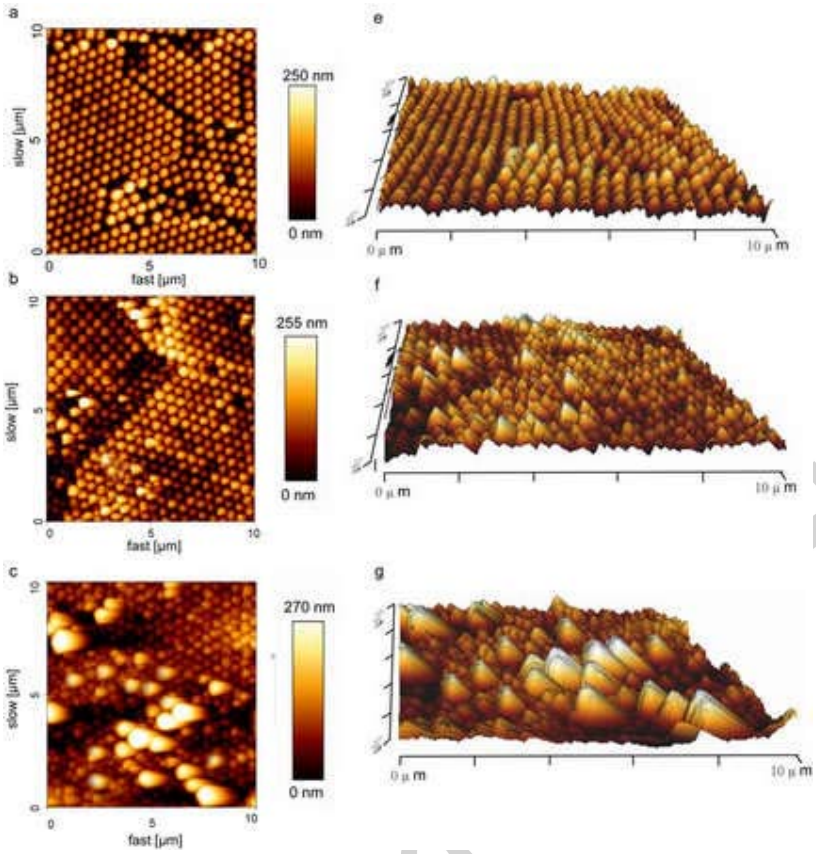

Fig.3. (Left) 10μm ×10μm 2-D AFM images of (a) bare MFON substrate (b) MFON substrate after modified with MS probes. (c) MFON substrate after incubation with target RNA(20 μL, 500nM at 37 °C for 8 hours). (Right) Panels (e), (f) and (g) are the representative 3-D AFM images of the 2-D images in (a), (b) and (c) respectively. The standard deviation of the AFM we used for experiment was about ±0.2 nm.

AFM technique allowed imaging of the same surface area throughout the MS probes immobilization and MS/RNA hybridization process. As it shown in Fig. 3a, the blank MFON substrate has a homogeneously surface with a height scale bar 0-250 nm; the average diameter of the nanopattern array is about 400 nm. Fig. 3b showed the substrate image after incubation with the MS probe (1 uM) for 120 minutes. In the image, a series of bright triangular morphology patterned on the surface (Fig. 3f) and the maximum height of the surface in the height scale bar increased to 255 nm, the average diameter of the nanopattern spots also increased to about 410 nm. These changes indicated the formation of the self-assembling of MS probes on the substrate. The MS probe was shown as triangular morphology in the image as the

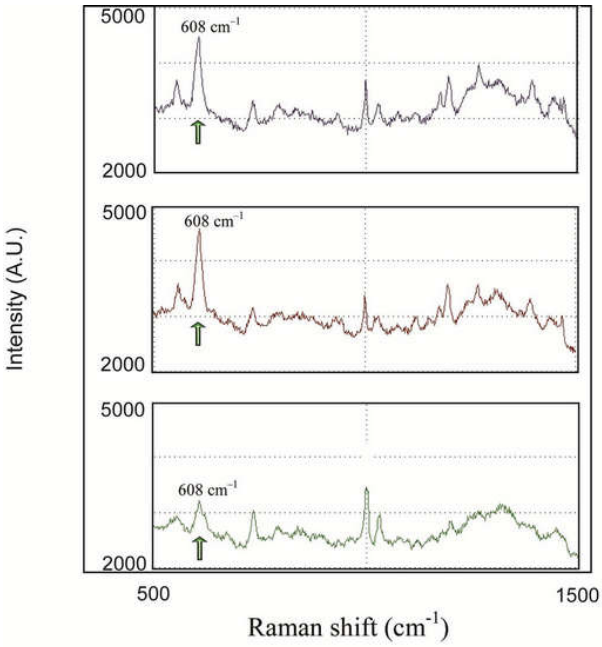

Fig.4. SERS spectra of MS-functionalized MFON substrates after incubation with blank sample, noncomplementary RNA sample and complementary target RNA sample at 37 °C for 8 hours.

flexible strand was hangover by the AFM needle-tip in the scanning process. The increase of the maximum height and the average diameter of the nanopattern illustrated that MS probes immobilized on the surfaces of the nanopattern and the gaps between of the nanopattern were slightly filled, increasing the diameter of the nanopattern as shown in Fig.3b. Fig.3c illustrated the MS-functionalized surface after incubation with the target RNA at a concentration of 0.5 μ M for 8 h at 37 °C. As it shown in the image, after incubation with the target RNA sample, much larger triquetrous apophasis appeared and the maximum height of the surface increased from 255 nm to 270 nm. The remarkable morphology expanding illustrated the hybridization between of the MS probe and RNA and the increase of the maximum height of the surface proved that the hairpin loop of the MS probe had been opened after hybridization with the target RNA. The change scope was consistent with the DNA self-assembling data reported before (Kelley et al., 1998; Mui et al., 2001).To further ensure the calibration of the system, the bare substrate (with no MS probes) was incubated in the RNA target solution (500nM RNA of 0.5 M NaCl and 10 mM PBS aqueous solutions) at 37 °C for 8h, washing 3 times with DI and then dried for AFM detection. Compared with the bare substrate image without RNA incubation as shown in Fig.3a, there was almost no difference. That means the effect induced to the AFM images by the nonspecifically absorption of the RNA or other elements on the surface can be eliminated.

3.4. SERS sensitivity detection of the RNA target sequences

The SERS signal response was detected after 8 h incubation of the MS-substrate at 37 °C with three types of RNA samples: the blank sample, 1 μ M non-complementary RNA sequence and 1 μ M complementary target RNA sequence respectively. As shown in fig. 4, the SERS at 608 cm^{-1} (Raman shift) was chosen as the signal peak of Cy-3 molecule to compare the SERS intensities of the three samples. For the blank sample, there was a distinct signal at 608 cm^{-1} as the Cy-3

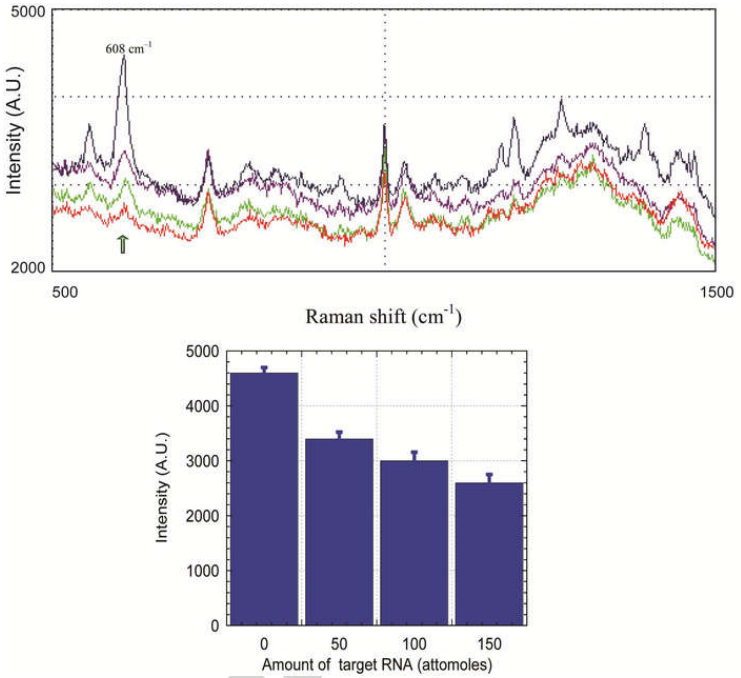

Fig.5. SERS spectra and intensity of the MS-functionalized MFON substrates after adding different amounts of complementary target RNA. Error bars: standard deviation (n =5). For each samples, SERS signals was collected from five different spots on the same chip (1×1 cm^2) and the five SERS spectra were averaged to represent the final SERS spectrum for each sample and the standard deviation was also calculated from the five detections for each sample.

molecule labeled on the 3′end of the MS probe was closed to the SERS surface. While the intensity difference between the non-complementary RNA sample and the blank is very small. For the complementary target RNA sample, the intensity at 608 cm^{-1} decreased about 30% compared with the blank. The decrease indicates that the target RNA sequences hybridized with the MS probes and opened the stem loops so that the Cy-3 dyes tagged at the 3′ end of the MS probes were separated from the SERS substrate. Considering the length of the target RNA sequence (33 nucleotides, approximately 10 nm), after hybridization, the distance of Raman label Cy-3 to the substrate was increased more than tenfold (the distance prior to hybridization was less than1 nm) so that SERS intensity will be decreased. As our SERS response was induced

by the hybridized RNA on the substrate, the excessive and non-hybridized RNA sequences will not induce false response spectra, so that post-hybridization washing step was not required. Compared with the common SERS-based DNA detection constitute of DNA-capture probe/DNA target/DNA reporter probe tripartite (Cao et al., 2013; Li et al., 2008) for which two-step hybridization and many steps washing were necessary, our method is simple and requires less reagent cost. To investigate the stability of our assay, the variability of the MS probes-modified

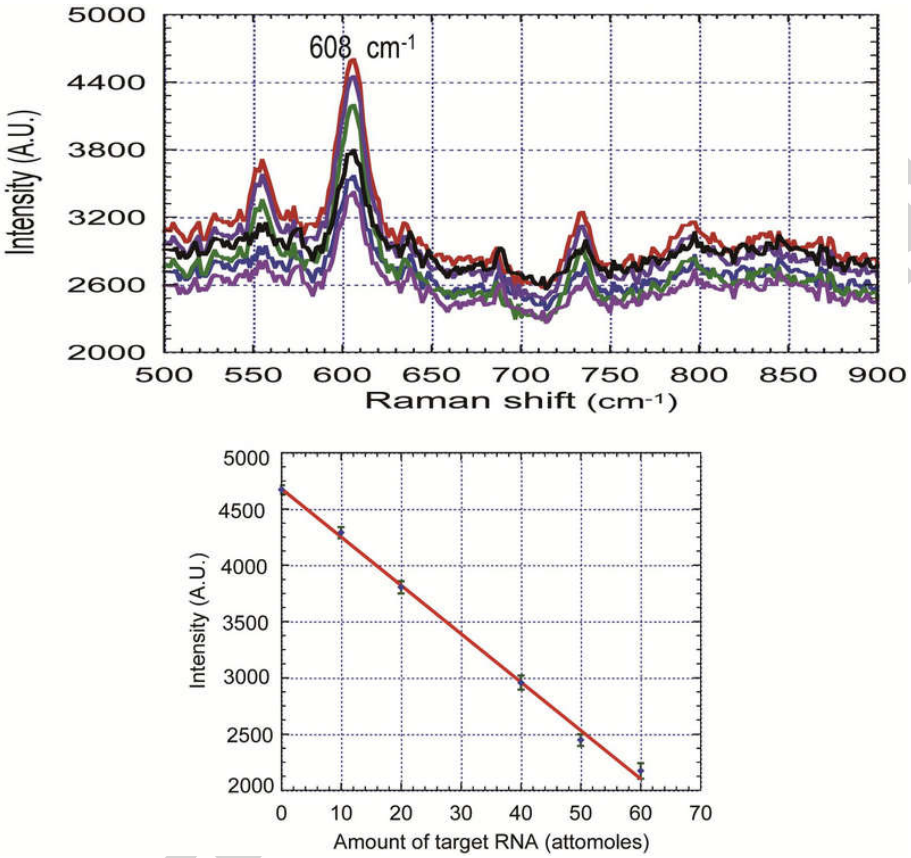

Fig. 6. SERS spectra of MS-functionalized MFON substrates at different amount of complementary target RNA from 0 to 60 attomoles and the linear relationship between the complementary target RNA amount and the SERS intensity in the range. Error bars: standard deviation (n =5). For each samples, SERS signals was collected from five different spots on the same chip (1×1 cm^2) and the five SERS spectra were averaged to represent the final SERS spectrum for each sample and the standard deviation was also calculated from the five detections for each sample.

substrate was assessed by calculating a coefficient of variation (CV). The chip CV was defined as dropping the same RNA sample on five small chips with the same region (1×1 cm^2) which were incised from the same large SERS substrate, ten SERS measurements were operated for each chip. The point CV was defined as dropping the same RNA sample on one small chip and the SERS signals focus on five different

points (with a laser spot of 10 μm in diameter) were collected, ten SERS measurements were operated for each point. Full details on CV calculation are provided in Table 2 in Supporting Information. For the same RAN sample, both of the chip CV and point CV were observed to be less than 10%.

In order to certify the possibility of the quantitative analysis by using this method, a series of target RNA samples (50 μL)with concentrations of 1 μM, 2 μM, and 3 μM was dropped on the SERS substrate chips respectively. Each 50 μL sample spread over the entire chip area of 1×1 cm^2. The laser beam spot of 10 μm excited only a minute fraction (10^{-6}) of the sample (only 50 picoliters). Thus, the amount of complementary target RNA excited by the focused laser spot is approximately 50 attomoles, 100 attomoles and 150 attomoles, respectively. As shown in the Fig.5, the SERS intensity decreases about 27% when RNA increasing from 0 to 50 attomoles and the decrease slows down to 9% and 7% when RNA increased from 50 to 100 attomoles and further from 100 to 150 attomoles. This result suggests that there may be linear dependence between of the RNA amount and the SERS signal in a limitative scope. To further determine the limit of detect, the linear relationship between the complementary target RNA and the SERS intensity was studied. We delivered 50 μL complementary target RNA samples with concentrations of 0.2 μM, 0.4 μM, 0.8 μM, 1 μM, 1.2 μM and 2 μM to the chips (1×1 cm^2)respectively, as it referred before, the amount of complementary target RNA excited by the focused laser spot is approximately 10, 20, 40, 50 ,60 and 100 attomoles respectively. For each samples, SERS signals was collected from five different spots on the same chip (1×1 cm^2) and the five SERS spectra were averaged to represent the final SERS spectrum for each sample and the standard deviation was also calculated from the five detections for each sample. As shown in Fig.6, the standard curve showed a good linear relationship with a correlation coefficient of 0.9950 and a very low LOD of 2.67 attomoles (The LOD value can be estimated by the equation $LOD=3\times S_{blank}/m$, in which S_{blank} and m are the standard deviation of the blank and the slope obtained from the linear fitting) in the linear relationship of 0-60 attomoles (The curve from 60 to 100 attomoles was not shown as the linear relationship is inconsistent). Compared with the other SERS-based RNA detection methods (nM-fM) recently reported (Abell et al., 2012; Negri et al., 2013), our assay can provide a higher sensitivity.

4. Conclusions

We have demonstrated a potential diagnostic tool for HPAI virus point-of-care early detection. By using the MS probes modified SERS substrate, the RNA target sequences coding for the N66S gene mutation in PB1-F2 protein linked to HPAI virus can be detected with a linear response over 0-60 attomoles and the LOD is 2.67 attomoles. With this assay, RNA transcripts extracted from as little as about 60000 cells (*e.g.* 10-100 copies per cell) can be detected directly without PCR amplification (Ballet et al., 2008; Duggan et al., 1999), which will liberate the HPAI virus diagnosis from laboratory to the point-of-care test. Future work will aim at developing a series MS

probes for the virus RNA marker besides HPAI and the MS probes will be expand from DNA to locked nucleic acid (LNA) or peptide nucleic acids (PNA) which possessed stronger binding affinity to RNA sequence. Novel SERS active substrate will also be studied to increase the sensitivity so that the cell samples from patients for practical clinical diagnosis can be decreased further.

Acknowledgments

This work is supported by the National Natural Science Foundation of China (No. 31100712)

References

Abell, J.L., Garren, J.M., Driskell, J.D., Tripp, R.A., Zhao, Y., 2012. J. Am. Chem. Soc. 134(31), 12889-12892.

Amano, Y., Cheng, Q., 2005. Anal. Bioanal. Chem. 381(1), 156-164.

Ballet, F., Bouma, M. E., Wang, S. R., Amit, N., Marais, J., Infante, R., 2008. Hepatology, 4(5), 849-854.

Barhoumi, A., Zhang, D. Tam, F., Halas, N. J., 2008. J. Am. Chem. Soc. 130(16), 5523-5529.

Barhoumi, A., Zhang, D., Halas, N. J., 2008. J. Am. Chem. Soc. 130(16), 14040-14041.

Beveridge, W. I. B., 1991. Hist. Philos. Life Sci. 13(2), 223-235.

Cao, Y.W.C., Jin, R.C., Mirkin, C.A., 2002. Science. 297(5586), 1536-1540.

Conenello, G.M., Zamarin, D., Perrone, L.A., Tumpey, T., Palese, P., 2007. PLoS Pathog. 3(10), 1414-1421.

Duggan, D.J., Bittner, M., Chen, Y., Meltzer, P., Trent, J. M., 1999. Nat. Genet. 21, 10-15.

Dybing, J. K., Schultz-Cherry, S., Swayne, D. E., Suarez, D. L., Perdue, M. L., 2000. J. Virol., 74(3), 1443-1450.

Fouchier, R.A.M., Bestebroer, T.M., Herfst, S., Rimmelzwaan, G.F., 2000. J. Clin. Microbiol. 38(11), 4096-4101.

Green, M.F., Liu, M., Cohen, L., Kollensperger, P., Cass, T., 2006. Faraday Discuss. 132, 269-280.

Hatta, M., Gao, P., Halfmann, P., Kawaoka, Y., 2001. Science. 293 (5536), 1840-1842.

Kang, T., Yoo, S.M., Yoon, I., Lee, S.Y., Kim, B., 2010. Nano Lett. 10 (4), 1189-1193.

Kash, J.C., Tumpey,T.M. Proll, S.C., Carter,V.O., Perwitasari, M.J., Thomas, C.F., Basler, P., Palese, J.K., Taubenberger, A., Swayne, D.E., Katze, M.G., 2006. Nature. 443, 578-581.Levin, C.S., Kundu, J., Barhoumi, A., Halas, N. J., 2009.

Analyst, 134 (9), 1745-1750.

Li, J.M., Ma, W.F., You, L.J., Guo, J., Hu, J., Wang, C.C., 2013. Langmuir. 29 (20), 6147-6155.

Li, M., Cushing, S.K., Liang, H., Suri, S., Ma, D., Wu, N., 2013. Anal. Chem. 85(4), 2072-2078.

Maiti, M., Nauwelaerts, K., Herdewijn, P., 2012. Bioorg. Med. Chem. Lett. 22(4), 1709-1711.

Mitchell, P.S., Parkin, R.K., Kroh, E.M., Fritz, B.R., Wyman, S. K., Pogosova-Agadjanyan, E.L., Peterson, A., Noteboom, J., O'Briant, K.C., Allen, A., Lin, D.W., Urban, N., Drescher, C. W., Knudsen, B.S., Stirewalt, D.L., Gentleman, R., Vessella, R. L., Nelson, P.S., Martin, D.B., Tewari, M., 2008. Proc. Natl. Acad. Sci. U.S.A., 105(30), 10513-10518.

Murata, A., Fukuzumi,T., Umemoto, S., Nakatani, K., 2013. Bioorg. Med. Chem. Lett. 23(5), 252-255.

Negri, P., Dluhy, R.A., 2013. Analyst. 138, 4877-4884.

Nguyen-Van-Tam, J.S., Hampson, A.W., 2003. Vaccine. 21(16), 1762-1768.

Ngo, H.T., Wang, H.N., Fales, A.M., Vo-Dinh, T., 2013. Anal. Chem. 85(13), 6378-6383.

Sam, M., Boon, E.M., Barton, J.K., Hill, M.G., Spain, E.M., 2001. Langmuir.17 (19), 5727-5730.

Shana O. Kelley,S.O., Jacqueline K. Barton,J.K., Nicole M. Jackson, N.M., Lee, D.M., Potter, A.B., Spain, E.M., Allen, M.J., Hill,M.G., 1998. Langmuir. 14(24), 6781-6784.

Smith, G.J.D., Vijaykrishna, D., Bahl, J., Lycett, S.J., Worobey, M., Pybus, O.G., Ma, S.K., Cheung, C.L., Raghwani, J., Bhatt, S., Peiris, J.S.M., Guan, Y., Rambaut, A., 2009. Nature. 459, 1122-1125.

Stiles, P.L., Dieringer, J.A., Shah, N.C., Van Duyne, R.P., 2008. Annu. Rev. Anal. Chem. 1(1), 601- 626.

Szretter, K.J., Gangappa, S., Lu, X., Smith, C., Shieh, W.J., Zaki, S.R., Sambhara, S., Tumpey, T.M., Katz, J.M., 2007. J Virol. 81(6), 2736-2744.

Wang, H.N., Dhawan, A., Du, Y., Vo-Dinh, T., 2013. Phys. Chem. Chem. Phys. 15, 6008-6015.

Wang, J.F., Dong, P. Di, D., Chen, J., Wang, C., Wang, H., Wu, X., 2013. J Nanoengineering and Nanosystems . 227(2), 57-62

Wang, Y., Lu, N., Wang, W., Liu, L., Feng, L., Zeng, Z., Li, H., Xu, W., Wu, Z., Hu, W., Lu, Y., Chi, L., 2013. Nano Research, 6(3) 159-166.

Wei, Y., Cao, C., Jin, R., Mirkin, C.A., 2002. Science. 297 1536-1539.

Wen, Y., Wang, W., Zhang, Z., Xu, L., Du, H., Zhang, X., Song, Y., 2013. Nanoscale, 5, 523-526.

Yuan, H., Liu, Y., Fales, A.M., Li, Y.L., Liu, J., Vo-Dinh, T., 2012. Anal. Chem. 85(1), 208-212.

Yuen, K.Y., Chan, P.K.S., Peiris, M., Tsang, D.N.C., Que, T.L., Shortridge, K.F., Cheung, P.T., Cheng, A.F.B., 1998. Lancet. 351(9101), 467-471.

Zhou, X., Zhou, F., Liu, H., Yang, L., Liu, J., 2013. Analyst.138, 5832-5838.

Highlights

- A molecular sentinel (MS) modified SERS biochip for RNA genetic marker of PB1-F2 protein in highly pathogenic avian influenza (HPAI) virus detection has been reported.
- A metal film over nanosphere (MFON) substrate has been made with a SERS enhancement of 1.7×10^5.
- The hairpin MS probes with Raman label tagged were immobilized on MFON substrate and a decrease of Raman intensity can be induced after target RNA added as the MS stem-loop configuration was opened.
- The characterization of the hairpin MS probes from stem-loop configuration (closed state) to MS/RNA hybridization configuration (open state) was monitored by Atomic Force Microscopy (AFM).
- This method is one-step reaction and no need no post-hybridization washing, the limit of detect is 2.67 attomoles, content for the potential applications for HPAI point-of-care diagnosis in resource-limited settings.